Jamming for nematic deposition in the presence of impurities

E. E. Vogel,[1,2,*] J. F. Valdes,[1] W. Lebrecht,[1] A. J. Ramirez-Pastor,[3] and P. Centres[3]
[1]*Departamento de Física, Universidad de La Frontera, Casilla 54-D, Temuco, Chile*
[2]*Center for the Development of Nanoscience and Nanotechnology (CEDENNA), 9170124 Santiago, Chile*
[3]*Departamento de Física, Instituto de Física Aplicada, Universidad Nacional de San Luis-CONICET, Ejército de Los Andes 950, D5700HHW, San Luis, Argentina*
(Received 15 November 2016; published 16 February 2017)

The deposition of one-dimensional objects (such as polymers) on a one-dimensional lattice with the presence of impurities is studied in order to find saturation conditions in what is known as jamming. Over a critical concentration of k-mers (polymers of length k), no further depositions are possible. Five different nematic (directional) depositions are considered: baseline, irreversible, configurational, loose-packing, and close-packing. Correspondingly, five jamming functions are found, and their dependencies on the length of the lattice, L, the concentration of impurities, $p = M/L$ (where M is the number of one-dimensional impurities), and the length of the k-mer (k) are established. In parallel, numeric simulations are performed to compare with the theoretical results. The emphasis is on trimers ($k = 3$) and p in the range [0.01,0.15], however other related cases are also considered and reported.

DOI: 10.1103/PhysRevE.95.022120

I. INTRODUCTION

The deposition of one-dimensional objects (such as polymers) usually cannot fully cover the lattice leaving empty positions in what is called jamming. An extensive overview of this field can be found in the excellent work by Evans [1] and references therein.

The blocking of the lattice by the deposited objects plays an important role in numerous systems in which the deposition process is irreversible over time scales of physical interest [2]. In this theoretical frame, anisotropic particles of different shapes and sizes have been studied: linear k-mers (particles occupying k adjacent lattice sites) [3–7], flexible polymers [8,9], T-shaped objects and crosses [10], squares [11–14], disks [15], regular and star polygons [16], etc. In all cases, the limiting or jamming coverage depends strongly on the shape and size of the depositing particles. This is the classical random sequential deposition (RSD) or random sequential adsorption (RSA) [17] that is usually invoked in catalysis, corrosion, and other surface science problems. Here we will consider other possible depositions as well.

The jamming phenomenon is enhanced by the presence of impurities that prevent the deposition of objects over them and some of the neighboring positions. Two previous articles from our group [18,19] were devoted to the study of percolation and jamming properties of extended objects deposited on square lattices with the presence of impurities. The simulations were performed for k-mer sizes ranging from 2 to 9. More recently, Tarasevich *et al.* [20] extended the study of straight rigid k-mers with defective sites to larger particle sizes (k values up to 128). For each value of k, the results showed the existence of a critical fraction of impurities, at which percolation threshold and jamming coverage are equal and, consequently, percolation becomes impossible.

The effects of impurities on percolation and jamming properties of straight rigid k-mers have also been studied for triangular lattices [21,22]. In these papers, the filling process was done in two stages. In the first stage, impurity particles were deposited up to some level. In the next stage, the k-mers were adsorbed on the substrate contaminated by impurities. The author showed how the size and impurity concentration affect the percolation threshold [21] and jamming coverage [22].

In the present paper, we study analytically and numerically the jamming problem varying the length of the k-mer (linear polymer of length k in terms of the lattice constant), the concentration of impurities, p, and the size of the square lattice, L, discussing the thermodynamic limit as $L \to \infty$.

We will consider below five different deposition cases: close-packing or attractive, loose-packing or repulsive, sequential irreversible (the usual deposition case described above), configurational (or equilibrium considering all possible configurations), and baseline configurational (a mathematical way of looking at this problem based on the jamming configurations only). These depositions will be carefully defined below.

We address here the very important case of directional nematic deposition where objects are lined up directionally at the moment of deposition. This is the case of guided deposition of oriented nanotubes [23] or magnetically oriented deposition of particles [24,25]. In the present case, we consider depositions of longitudinal objects along one given direction ("horizontal"), which coincides with the axis of the k-mer. Transverse depositions at any angle are inhibited by external conditions (flux, electric fields, magnetic fields) appropriate for each kind of polymer. This nematic deposition actually uncouples in the vertical direction from the horizontal direction since depositions along the former are forbidden, so each row is independent. This simplification allows us to consider depositions on any one of the rows of the square lattice, which is equivalent to a one-dimensional lattice (ODL).

In addition, we consider the presence of impurities randomly spread all over the ODL. This is illustrated in Fig. 1 for a random location of impurities (a) and for an equally spaced deposition of impurities (b). Such impurities prevent the deposition of any portion of the k-mer over them, so

*Corresponding author: eugenio.vogel@ufrontera.cl

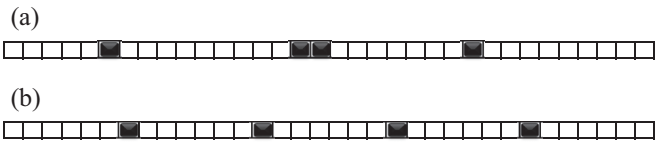

FIG. 1. Two possible distributions for four one-site impurities on an $L = 34$ one-dimensional lattice. (a) A random distribution with one segment of nil length (two impurities touching each other); (b) an equally spaced distribution with all segments of length 6.

such depositions can occur only within segments between impurities. Let us call ℓ the length of a particular segment; then depositions of k-mers with $k \leqslant \ell$ are possible. We will begin by finding the jamming conditions for segments of finite length ℓ.

It is well known that it is quite a difficult matter to analytically determine the value of the jamming coverage for a given lattice. For some special types of lattices, geometrical considerations enable us to derive their jamming thresholds exactly. In the case of straight rigid k-mers on an ODL of length L under periodic boundary conditions (mimicking the thermodynamic limit), the RSA problem has been solved exactly [3,26], leading to

$$\theta^k_{L\to\infty}(t) = k\int_0^t \exp\left[-u - 2\sum_{j=1}^{k-1}\left(\frac{1-e^{-ju}}{j}\right)\right]du, \quad (1)$$

where $\theta^k_L(t)$ represents the fraction of lattice sites covered at time t by the deposited k-mers. However, in the present case we consider finite impurity concentrations p, which necessarily partitions the lattice into finite segments between consecutive impurities even in the thermodynamic limit. So a new derivation of the jamming condition valid for fixed ends in now necessary. This is done in the Appendix at the end of this paper.

Parameters k, ℓ, and L (measured in lattice constants) will be varied, but the length of the deposited object k is kept constant during the deposition process. In other words, no mixing of depositing objects of different length will be allowed. Concentration p is related to ℓ as we show below, so it is also varied.

In this work, we investigate the jamming phenomenon in the presence of impurities for the case of nematic deposition of straight rigid k-mers. Impurities are supposed to present a random distribution, which generalizes the treatment. We consider in detail the deposition of k-mers over linear segments of different finite sizes. The simultaneous consideration of five different deposition cases enriches the study and leads to interesting results to understand the jamming problem.

The paper is organized as follows: in Sec. II, the basic definitions are given, the general basis for the computer simulations are established, and the five deposition cases are defined. Results for the lattices with impurities are presented and discussed in Sec. III; relevant results for finite segments are given in the Appendix. Finally, the conclusions are drawn in Sec. IV.

II. THE MODEL

A. The system

As explained above, we only need to consider one row of the lattice at a time, which reduces the problem to the deposition of k-mers on an ODL of length L that has M impurities of length 1 on it. Then the concentration of impurities p is given by

$$p = \frac{M}{L}. \quad (2)$$

In principle, impurities can occupy any lattice site; consecutive impurities will act as impurities of larger extension. A total of M single impurities spread across a lattice of length L produces $N = M + 1$ segments of lengths $\ell_1,\ell_2,\ldots,\ell_i,\ldots,\ell_N$. An example is shown in Fig. 1(a) for noninteracting impurities for the case $M = 4$ and $L = 34$. If two impurities are next to each other, the length of the segment in between is zero. Figure 1(b) presents the case in which impurities are uniformly distributed within the ODL (which would be the case for highly self-repulsive impurities).

Generally speaking, the average segment length is given by

$$\langle\ell\rangle = \frac{\sum_{i=1}^N \ell_i}{N} = \frac{L-M}{M+1} = \frac{1-p}{p+1/L}, \quad (3)$$

which establishes a relationship between ℓ and p for each different L.

In the thermodynamic limit, this is equivalent to

$$\langle\ell\rangle_{L\to\infty} = \frac{1-p}{p}, \quad (4)$$

which is a finite value. The length of the segments has to be considered as a finite value, so the approximation of periodic boundary conditions [3] to calculate the jamming coverage does not apply here.

The concentration of impurities considered below will be in the range [0.01,0.15]. Lower concentrations correspond to very diluted impurities with negligible effect. Larger concentrations of impurities lead to interesting problems of their own, but they are beyond the scope of this paper. The numeric simulations below will be for lattices with $L \geqslant 1000$, where Eq. (4) is good enough.

A random distribution of impurities can produce a huge variety of combinations, producing segments of different lengths; in other words, there is a distribution of lengths for the segments. Segment number 1, for instance, is defined by the wall to the left, an impurity with probability p at the right end, and $\ell_i = i$ consecutive empty sites in between with a probability $(1-p)$ each; the total probability for such a segment is $p(1-p)^i$.

It can be noticed that these probabilities are normalized:

$$\sum_{i=0}^{i_{\max}} p(1-p)^i \approx \sum_{i=0}^{\infty} p(1-p)^i = p + p\frac{1-p}{1-(1-p)} = 1. \quad (5)$$

Then, the number of segments of length i, denoted by s_i, can be written as

$$s_i \approx p(1-p)^i(pL+1), \quad (6)$$

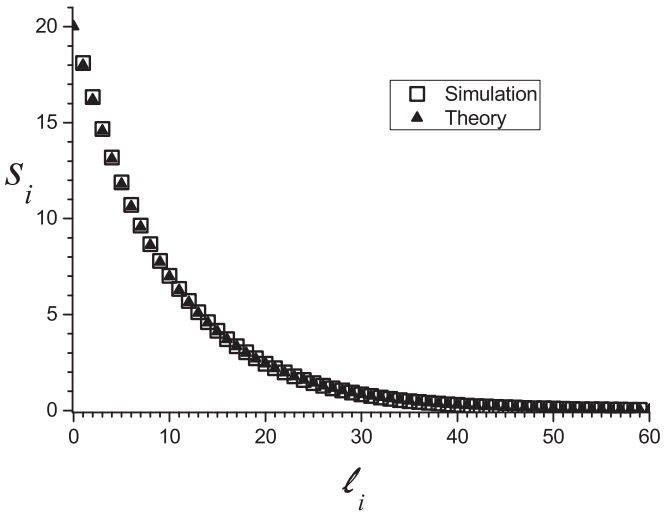

FIG. 2. Segment length distribution for $L = 2000$, $M = 200$ ($p = 0.10$); average values after 1000 initializations.

where $(pL + 1)$ is the total number of segments for a lattice of length L and impurity concentration p.

The function in Eq. (6) is plotted by means of solid triangles in Fig. 2, where numbers are adapted to represent results over a lattice $L = 2000$ and $p = 0.1$ ($\ell_i = i$). Theoretical results are compared with simulation data. The numerical example for $L = 2000$ considers $M = 200$ impurities ($p = 0.1$), namely 201 segments (eventually some of them of length zero). These results are represented by means of open squares in Fig. 2 after 1000 independent initializations, meaning a total of 201 000 segments.

The average segment in this exercise is $\langle \ell \rangle = 8.96$, which is about what can be expected since the thermodynamic limit for this value is $\langle \ell \rangle = 9.0$ according to Eq. (4). Similar calculations can be done for other concentrations as presented in Fig. 3. For the impurity concentrations considered here, we shall use the results of Eq. (4) as the average segment length for the impurity concentration p in the rest of the paper.

A careful scrutiny of Fig. 2 indicates that there are segments shorter than the size of the k-mer that are bound to remain empty after the impurity occupation of the lattice. The total number of such blocked positions due to segments shorter than k depends mainly on k, and it is given by

$$B_p^k = \sum_{i=1}^{k-1} i \times s_i. \tag{7}$$

Then, the total number of unblocked positions within the ODL available for depositions of k-mers is

$$\Upsilon_p^k = L - M - B_p^k. \tag{8}$$

The fraction of the lattice available for k-mer depositions is $\upsilon_p^k = \Upsilon_p^k / L$, namely

$$\upsilon_p^k = 1 - p - \beta_p^k, \tag{9}$$

where

$$\beta_p^k = \frac{1}{L} \sum_{i=1}^{k-1} i \times s_i. \tag{10}$$

The fraction of the lattice available for k-mer depositions is given by Eq. (9) and it is plotted with respect to p in Fig. 4 for dimers ($k = 2$) and trimers ($k = 3$). As in Fig. 2, these simulations correspond to $L = 2000$, $M = 200$ ($p = 0.1$), and 1000 independent initializations.

Thus, υ_p^k acts as an upper limit for the concentration reached due to k-mer deposition in a lattice with impurity concentration p. No matter how efficient the deposition method can be, υ_p^k cannot be overcome.

As depositions of k-mers take place, the number of occupied positions at a certain moment is nk, and it continues to increase up to the deposition of the last possible k-mer, for $n = w(p)$ say, giving a maximum number of $w(p)\,k \leqslant \Upsilon_p^k$ positions

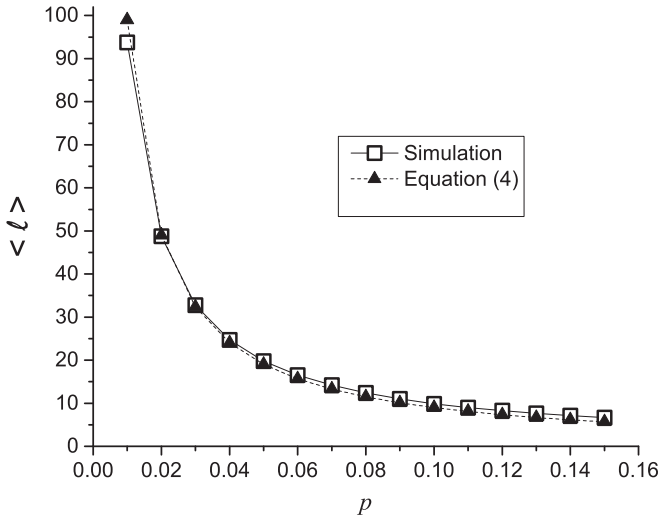

FIG. 3. Average segment length as a function of impurity content for $L = 2000$ (solid triangles), compared to the average segment length for a system where $L \to \infty$ (open squares).

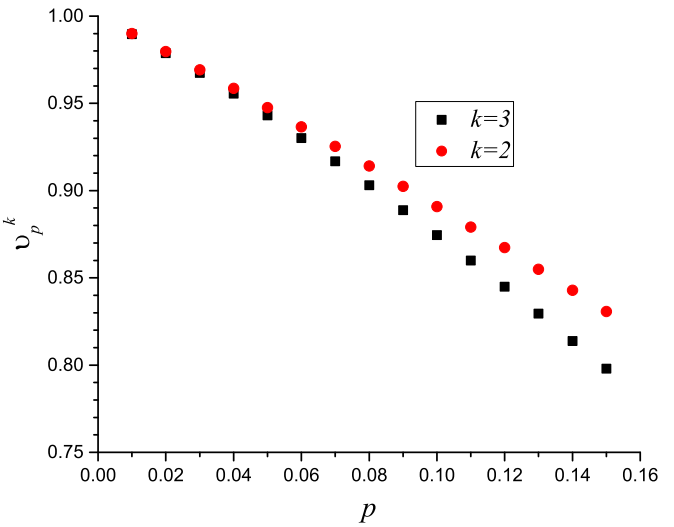

FIG. 4. Unoccupied portion of the ODL by means of blocking analysis: υ_p^k for $k = 2$ and 3 after simulations for $L = 2000$.

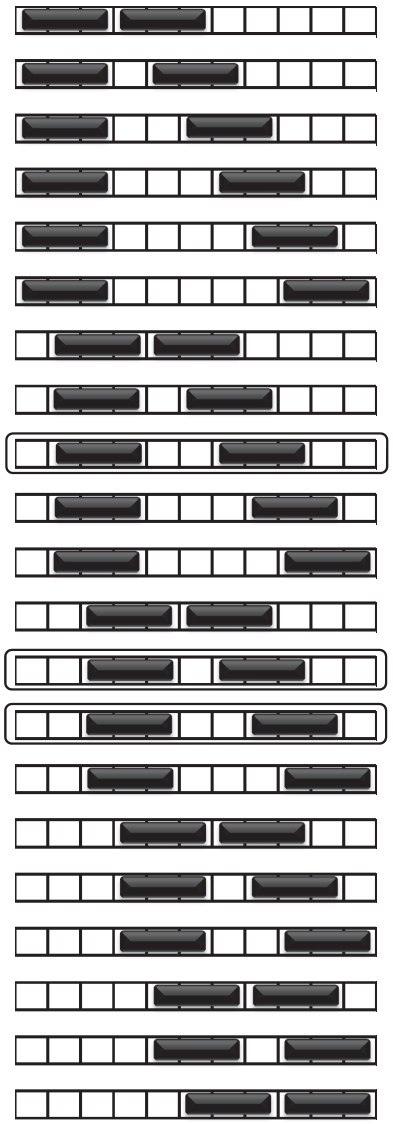

FIG. 5. All possible 21 depositions of two trimers within a segment of length 11. Just three of them lead to jamming; they are marked by an external rectangle. All other 18 depositions accept one more trimer.

finally occupied by k-mers. The coverage is then defined by

$$\Gamma_p^k = \frac{w(p)k}{L} \leqslant \upsilon_p^k. \tag{11}$$

B. Deposition cases

For any segment of length ℓ there is a jamming coverage for depositions of k-mers, which will be denoted by γ_ℓ^k in a generic way. We will discuss below five different functions γ_ℓ^k corresponding to five different deposition cases over segments.

Depositions occur on any segment in the lattice. We concentrate on a particular segment of length ℓ for which we will obtain all configurations with special attention over those that jam the segment. We will illustrate the process with an example for $\ell = 11$, as is shown in Fig. 5, where the 21 different ways in which two trimers can be deployed are presented. No overlaps are allowed, and all possible combinations of k-mers and empty spaces are considered. The three configurations presenting jamming are marked by a rectangle surrounding the segment. Such configurations will be referred to as jamming configurations.

When the deposition of three trimers is considered on a segment of length 11 (not shown), all the 10 possible distributions lead to jamming. Obviously, four trimers on a segment of length 11 is out of question. On the other extreme, there is no way in which just one trimer can jam a segment of length 11. For any segment of length ℓ, there is a minimum number of k-mers leading to jamming, u say; there is also a maximum number z of k-mers that can be accommodated in such a segment; $u = 2$ and $z = 3$ for the example with $\ell = 11$.

Generally speaking, a segment of length ℓ will present $d_\ell^{n,k}$ possible distributions or configurations of n k-mers within a segment of length ℓ:

$$d_\ell^{n,k} = \frac{(n + \ell - nk)!}{n!(\ell - nk)!} = \left(\frac{7!}{2!5!} = 21\right), \tag{12}$$

where $nk \leqslant \ell$. The result given in parentheses corresponds to the example of two trimers in a segment of length 11 just presented above.

The corresponding result for three trimers on a segment of length 11 is given by

$$d_{11}^{3,3} = \frac{5!}{3!2!} = 10. \tag{13}$$

Not all the possible configurations jam the system. We can denote by $j_\ell^{n,k}$ the number of jamming configurations for a segment of length ℓ and deposition of n k-mers. Thus, for the example under consideration, we have $j_{11}^{2,3} = 3$ and $j_{11}^{3,3} = 10$.

The corresponding coverage is obtained from the number of deposited k-mers, namely

$$x_\ell^{n,k} = \frac{nk}{\ell}. \tag{14}$$

We introduce now five different deposition conditions. The leading three correspond to noninteracting k-mers, while the last two represent cases of interacting k-mers.

1. Baseline deposition

This is a rather mathematical condition in which all jamming configurations have the same probability, regardless of any physical way in which this is reached. Although it is difficult to realize how it could be achieved experimentally, it serves as a general guide to the subject and a comparison point for the other realistic cases discussed next. Since it leads to the lowest possible jamming values for noninteracting k-mers, we call it "baseline".

For the case of homogeneous k-mer deposition, k is a fixed parameter in each experiment. The total number of jamming configurations is given by

$$J_\ell^k = \sum_{n=u}^{z} j_\ell^{n,k}, \tag{15}$$

where u and z were defined a few lines before Eq. (12) during the presentation of the example above.

The probability $P_\ell^{n,k}$ of jamming with n k-mers in this case is given by

$$P_\ell^{n,k} = \frac{j_\ell^{n,k}}{J_\ell^k}. \tag{16}$$

Then, the saturation concentration σ_ℓ^k is reached through the configurational probability:

$$\gamma_\ell^k = \sigma_\ell^k = \sum_{n=u}^{z} P_\ell^{n,k} x_\ell^{n,k}, \tag{17}$$

where $x_\ell^{n,k}$ is the site occupation for n polymers of length k. For the example under consideration with a total of 13 jamming configurations, we get

$$\sigma_{11}^3 = \tfrac{3}{13} \times \tfrac{6}{11} + \tfrac{10}{13} \times \tfrac{9}{11} = 0.755. \tag{18}$$

In the Appendix, we illustrate the way coefficients $P_\ell^{n,k}$ can be obtained for this deposition case. The extension to the other deposition cases is straightforward.

The jamming function for a segment of length ℓ for this deposition case will be denoted by σ_ℓ^k. The jamming function for the ODL with impurity concentration p will be denoted by $S^k(p)$ when defined below. The notation is as follows: lower-case Greek letters for segment jamming functions and upper case letters for lattice jamming functions.

2. Irreversible sequential deposition

This is the most common approach to jamming, which was already discussed in the Introduction as RSD. A protocol is defined in which a random site in the segment is picked, then a k-mer is applied from this pivot site along a previously assigned direction (left or right). If all these k sites are empty, the k-mer is deposited irreversibly. If at least one site is occupied by an impurity or a previous k-mer, a new pivot site is picked. The process continues until all possibilities are covered and all empty chains have lengths less than k. This deposition is dependent on the sequence in which the sites are occupied. This case will be studied numerically only as described below in a detailed way yielding the jamming function $\gamma_\ell^k = \theta_\ell^k$ for segments. The corresponding jamming function for the whole lattice will be denoted by $T^k(p)$.

3. Configurational deposition

In this case, all possible configurations for k-mer depositions are considered with equal probability. Jamming is studied for each k-mer concentration defined by n polymers of length k as given by Eq. (14). This deposition is not dependent on the sequence in which the k-mers are deposited since all possible accommodations are in principle possible. However, the configurations with extreme x values have low probabilities.

For a segment of length ℓ, the probability $Q_\ell^{n,k}$ for jamming is now given with respect to all possible configurations for that number n of k-mers (not over the total number of jamming configurations, as in Sec. II B 1), namely

$$Q_\ell^{n,k} = \frac{j_\ell^{n,k}}{d_\ell^{n,k}}. \tag{19}$$

The no jamming probability or complementary probability can be denoted as

$$C_\ell^{n,k} = 1 - Q_\ell^{n,k}. \tag{20}$$

Then, the total jamming function has to be calculated progressively now since configurations are tried on the basis of one at a time. For simplicity, we drop indices ℓ and k in the derivation of the jamming function ϕ_ℓ^k in the next lines. The first jamming possibility comes for $n = u$ with a probability Q^u and a coverage x^u, while the probability that the jamming occurs for any higher k value is the complementary probability (C^u). If this is the case, configurations with one more k-mer are invited with a jamming probability $Q^{u+1,k}$ and a coverage x^{u+1}; the probability of not finding jamming at this stage is given by C^{u+1}. The process goes on for configurations with additional k-mers $(u+2, u+3, \dots)$ while jamming is not achieved. This continuous process ends when we reach the last possible configuration with a probability Q^z and a coverage x^z; the corresponding $C^z = 0$. This can be expressed in the following way recovering the full notation:

$$\begin{aligned}\phi_\ell^k = {} & Q_\ell^{u,k} x_\ell^{u,k} + C_\ell^{u,k}\big[Q_\ell^{u+1,k} x_\ell^{u+1,k} \\ & + C_\ell^{u+1,k}\big(Q_\ell^{u+2,k} x_\ell^{u+2,k} \cdots + C_\ell^{z-1,k} Q_\ell^{z,k} x_\ell^{z,k}\big)\big].\end{aligned} \tag{21}$$

For the example under consideration, we find

$$\begin{aligned}\phi_{11}^3 &= Q_{11}^{2,3} \times x_{11}^{2,3} + \big(1 - Q_{11}^{2,3}\big) Q_{11}^{3,3} \times x_{11}^{3,3} \\ &= \tfrac{3}{21} \times \tfrac{6}{11} + \tfrac{18}{21} \times \tfrac{10}{10} \times \tfrac{9}{11} = 0.779.\end{aligned} \tag{22}$$

The jamming function for segments is $\gamma_\ell^k = \phi_\ell^k$; the corresponding jamming function for the entire lattice will be denoted by $F^k(p)$.

For a textbook comparison between irreversible sequential deposition and configurational deposition, see [27]. In particular, the example in Sec. II B 1 is appropriate to the present discussion.

4. Loose packing or repulsive deposition

In this case, the k-mers can move while trying to stay apart within the segment. They repel each other and they could also repel the boundaries of the segment. This deposition can be realized by means of electrically charged (or ionized) segments. An acceptable deposition attempt finishes when equilibrium is reached and the repulsive energy reaches a minimum. Then configurations with one additional k-mer are attempted. The packing is loose since the spacing between k-mers is maximum, producing $n+1$ spaces of length up to $(k-1)$. In this case, the only possible configuration is the one with $n = u$, which leads to the repulsive jamming function:

$$\rho_\ell^k = x_\ell^{u,k}. \tag{23}$$

For the running example, this yields

$$\rho_{11}^3 = x_{11}^{2,3} = 0.545. \tag{24}$$

The jamming function for segments is denoted by $\rho_\ell^k = x_\ell^{u,k}$, while the corresponding one for the whole lattice will be denoted as $R^k(p)$.

5. Close packing or attractive deposition

In this case, the k-mers can move while trying to stay together within the segment. They attract each other and they could also attract the boundaries of the segment. This deposition can be achieved by electrically or magnetically polarized polymers properly oriented by external fields. An acceptable deposition attempt finishes when equilibrium is reached and the attractive energy reaches a minimum. Then, configurations with one additional k-mer are attempted. The packing is close since spacing between the n k-mers is minimum, ideally leaving just one space of maximum length $(k-1)$ depending on the commensuration with ℓ. The attractive jamming function is now given by

$$\alpha_\ell^k = x_\ell^{z,k}. \tag{25}$$

For the running example, this yields

$$\alpha_{11}^3 = x_{11}^{3,3} = 0.818. \tag{26}$$

The jamming function for segments is denoted by $\gamma_\ell^k = \alpha_\ell^k$ while the corresponding one for the whole lattice is $A^k(p)$.

III. RESULTS

A. Segments

With the aid of tables constructed according to the procedure described in the Appendix, we can obtain the jamming functions ϕ_ℓ^k, σ_ℓ^k, ρ_ℓ^k, and α_ℓ^k, according to the deposition case. Thus, for trimer occupation these four functions are given in Fig. 6 with respect to ℓ^{-1}. It is interesting to notice that for $\ell^{-1} = 0.125$ ($\ell = 8$), $u = z = 2$, so this is a common point for all depositions. From there onto higher values of ℓ, they split and show large differences.

In the case of θ_ℓ^k, the values shown in Fig. 6 were obtained using numerical simulations. In the filling process, straight rigid rods of size k ($k = 3$) were deposited randomly, sequentially, and irreversibly on an initially empty segment of length ℓ. The procedure of deposition is as follows: (i) one of the two possible lattice directions (left or right) and a starting site are randomly chosen; (ii) if, beginning at the chosen site, there are k consecutive empty sites, then a k-mer is deposited on those sites. Otherwise, the attempt is rejected. As is standard in the literature [28], the dimensionless time variable t was defined in terms of the number of deposition attempts per lattice site. For an ℓ-site segment, the time step $\Delta t = 1$ corresponds to ℓ deposition attempts. The jamming coverage is reached when it is not possible to deposit any more k-mers on the segment, this limit is reached for $t \approx 10^2$. Each point in the figure was calculated by averaging over 100 000 independent runs.

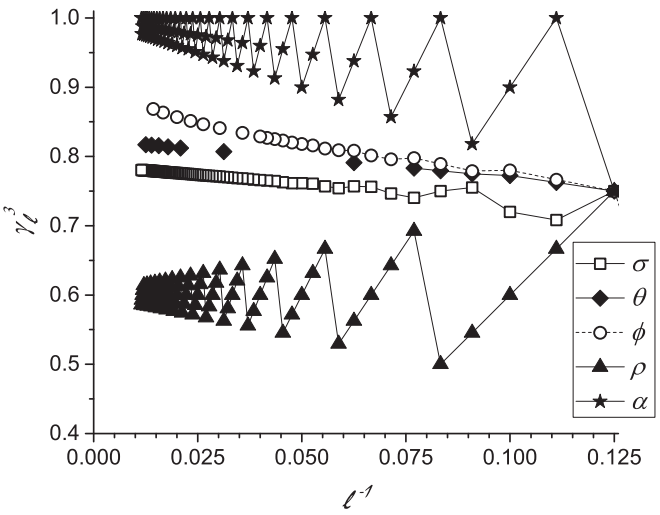

FIG. 6. Jamming concentrations γ_ℓ^3 as labeled in the inset where indices are omitted. Depositions correspond to trimers over segments of increasing length up to $\ell = 87$.

One interesting corollary coming from this exercise is that oscillations affect the results for the noninteracting depositions for small values of ℓ. In terms of their presence in the lattice of length L, Eqs. (2) and (3) indicate that this corresponds to a high impurity presence. For low impurity content, $p < 0.10$ say, oscillations lose importance, and linear regressions to extrapolate for the different γ functions are possible.

The oscillations of α are easy to understand since they are directly related to the commensuration properties of the k-mer with respect to ℓ. Whenever the latter is a perfect multiple nk of the former, $\alpha = 1.0$. As ℓ grows from here, α decreases reaching its local minimum at $\ell = nk + (k-1)$. Obviously in the thermodynamic limit these oscillations tend to disappear and $\alpha_\infty^k = 1.0$.

On the other extreme, the oscillations of ρ are related to the distribution of k-mers and spaces. In the case of lower coverage, the segment is covered by n k-mers of length k plus $n+1$ spaces of length $k-1$, namely $\ell = nk + (n+1)(k-1)$; the corresponding coverage nk/ℓ is $\rho_\infty^k = k/(2k-1)$ in the thermodynamic limit. In the case of higher coverage, there are n k-mers of length k and $n-1$ spaces, $\ell = nk + (n-1)(k-1)$, and the thermodynamic limit is again $\rho_\infty^k = k/(2k-1)$. This tendency is confirmed by Fig. 6 in the case of trimers. Cycles have a period $2k-1$ reflecting the addition of one k-mer and one large space of length $k-1$. This is reflected in Fig. 6 by a period 5 for trimers. As k increases, oscillations are more pronounced.

Values of ϕ_ℓ^k are larger than the corresponding ones for θ_ℓ^k due to the deposition sequence dependence of the latter. Let us use the example with $\ell = 11$ in Fig. 5 to understand this result. If we enumerate the configurations from top to bottom, we realize that the six leading ones lead to a jamming with three trimers. If we continue to the next five, where the first site of the segment is left empty, we realize that four of them jam with three trimers while the ninth one saturates with only two trimers, at a lower coverage. When we continue to the next four configurations (with two empty sites on the left end), half of them jam at the lower coverage. Since the deposition is irreversible, these three early jamming depositions will favor lower jamming concentrations. In the configurational deposition, these three jamming configurations have a weight but still there is a probability of reaching jamming at higher coverage. As ℓ grows, the difference between ϕ_ℓ^k and θ_ℓ^k is more notorious due to the increase in the number of possible configurations.

Another way of looking at these differences is to pay attention to the spectral distribution of results for the saturation coverage of θ_ℓ^k over a large number of initializations. This

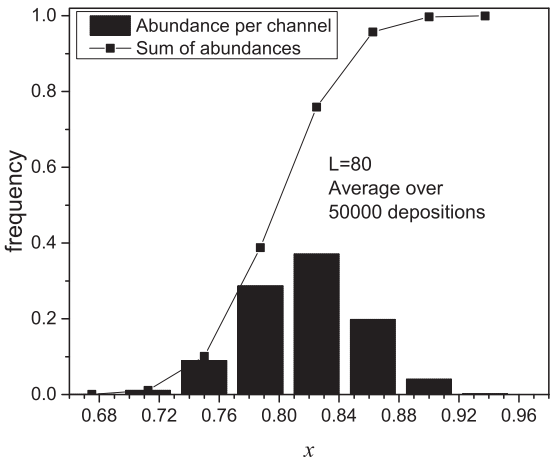

FIG. 7. Distribution for the jamming values for RSD after 50 000 depositions ($x = 3n/\ell$, where n is the number of saturating trimers) over a segment of length $L = \ell = 80$ (no impurities).

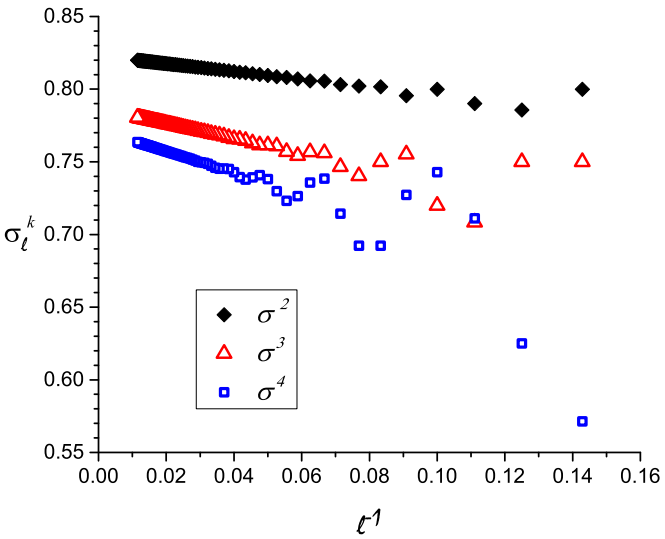

FIG. 8. Jamming function σ_ℓ^k for $k = 2$, 3, and 4 for the baseline deposition as functions of the segment length.

is done for trimers in Fig. 7 for $L = \ell = 80$, with 50 000 initializations. The distribution maximizes at $x_{80}^3 \approx 0.82$, corresponding to 22 trimers. Several comments are in order. First, the distribution is not symmetric with a tendency to favor jamming at lower coverage values. Second, it is a wide distribution going from about $x = 0.70$ to about $x = 0.90$ (both of these concentrations present a few samples from the 50 000 initializations). Third, upon looking at Fig. 6 we find that for $\ell^{-1} = 0.0125$ ($\ell = 80$) this distribution maximizes at θ_{80}^3; the left wing (lower x) of the distribution clearly includes σ_{80}^3 while the right side (higher x) of the distribution includes ϕ_{80}^3. Fourth, functions σ_ℓ^3 and ϕ_ℓ^3 escort the central θ_ℓ^3 jamming function for all values of ℓ, hence all values of p.

The baseline function σ_ℓ^3 necessarily goes under θ_ℓ^3 since the lower coverage jamming configurations are weighted with respect to other jamming configurations only. So, from this point of view σ_ℓ^k serves as a kind of lower bound for the distribution of possible jamming coverage configurations of noninteracting k-mers. The main advantage of σ_ℓ^k is that it is easy to calculate from an analytic point of view, so it can be used as a reference value.

The dependence on k can be appreciated in Fig. 8, where we have picked the baseline deposition for simplicity. As the length of the depositing polymer increases, strong oscillations occur for short segments or high impurity content. For a particular application involving long k-mers and/or high impurity content, some of these projections may not hold and a particular study should be done calculating the jamming conditions for each p and not by means of the linear regressions that will be used below in the case of trimers.

B. One-dimensional lattice with impurities

Finally, we turn our attention to the complete lattice with impurity concentration p. The aim is to find the five jamming functions $S^k(p)$, $T^k(p)$, $F^k(p)$, $R^k(p)$, and $A^k(p)$. They will be obtained from the γ jamming functions for segments for each deposition case and the impurity presence, which is a general feature independent of the deposition mechanism.

For the different depositions, we can plot the corresponding γ functions in the way presented in Fig. 6. Actually, we can obtain the linear regression in terms of ℓ^{-1} in each case. We have seen that $\langle\ell\rangle$ and p are related by Eq. (4). At this point, we propose to use $\langle\ell\rangle$ as representative of the distribution of lengths for a given p. This allows us to establish a direct connection between $\ell = \langle\ell\rangle$ and p.

Then we can express the linear regressions for the γ's in terms of p, yielding

$$\sigma_p^3 = 0.78 - 0.53\,p, \tag{27}$$

$$\theta_p^3 = 0.84 - 0.59\,p, \tag{28}$$

$$\phi_p^3 = 0.88 - 0.66\,p, \tag{29}$$

$$\rho_p^3 = 0.6, \tag{30}$$

and

$$\alpha_p^3 = 1.0 - 1.097\,p. \tag{31}$$

In the last two cases, we attempt a description of the general tendency only avoiding the oscillations related to the k-mer length, i.e., we pay attention to the central point only. In the case of the repulsive depositions, the central point lays on a constant line at 0.6. In the case of the attractive interaction, the straight line given by the last equation was obtained from the central points of α_p^3 in Fig. 6.

We now combine these results, that are valid for segments, with a previous analysis on the available portion of the lattice over which depositions are possible, as discussed in connection with Eq. (8) and Figs. 2 and 4. Three different mechanisms act to limit the jamming functions: (i) The impurity concentration p on its own, which is deposition-independent; (ii) the blocked positions, which depend on both p and k, as discussed in connection with Fig. 4 and its discussion; this is also deposition-independent; and (iii) the deposition of the k-mers

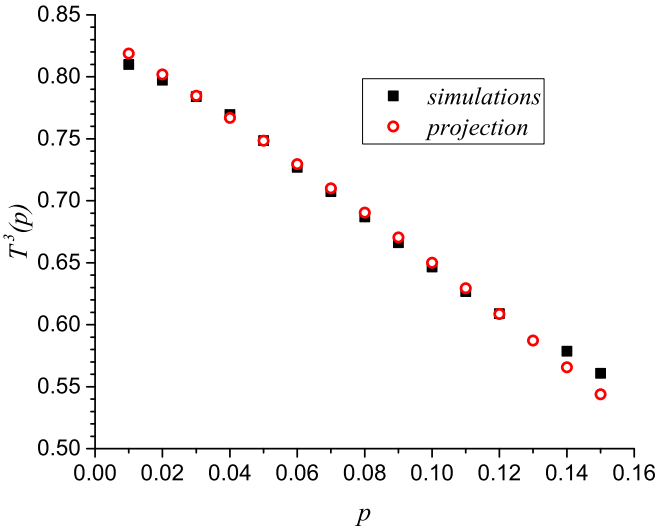

FIG. 9. Jamming function for the full lattice for trimer irreversible deposition. Red circles are obtained from Eq. (32) in the text, corresponding to a projected result from previously simulated depositions on segments. Black squares correspond to direct irreversible deposition of trimers over a whole lattice with $L = 10\,000$ for impurity concentration p.

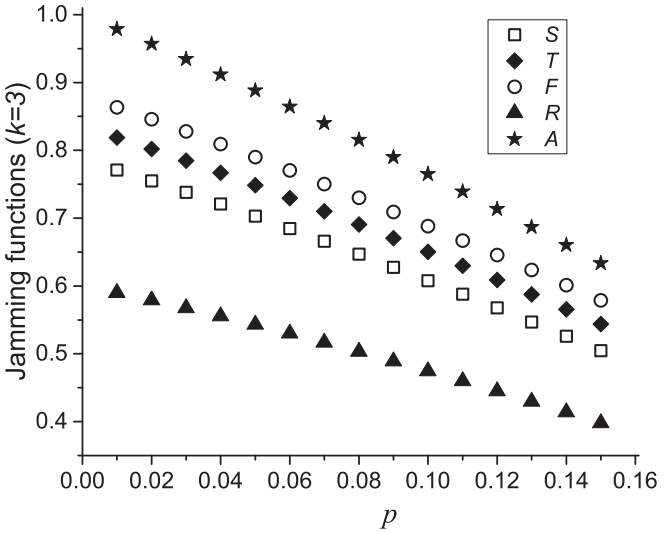

FIG. 10. Projected jamming functions for trimers on ODLs with impurity concentration p for the five depositions indicated in the inset.

within the segment, which is dependent on the way the polymers are deposited in the way shown by Fig. 6.

For the purpose of a comparative study among deposition mechanisms, we look for a representative way to describe the distribution in the last of the previous contributions to the jamming. We choose to use the average segment $\langle \ell \rangle$ due to its direct connection with p. The only justification we can give at the moment is that the projected results obtained in this way for $T^3(p)$ are in good agreement with those obtained by numeric simulations, as presented in Fig. 9. We are not guaranteed that such a good agreement holds for all deposition methods in the same way, but for comparative purposes it looks reasonable.

Then, jamming coverage functions for trimer depositions over an ODL with impurity concentration p for irreversible sequential deposition including the three previously identified contributions can be written as

$$T^3(p) = \theta_p^3 - p - \beta_p^3, \tag{32}$$

where β_p^3 has been obtained from numeric studies as presented in Fig. 4. In any case, β_p^3 starts at 0.0 for small p values and grows up to slightly over 0.05 for $p = 0.15$. We call the result given by Eq. (32) a projected result for $T^3(p)$ since it projects the result that is valid for segments to the entire lattice.

In Fig. 9, we compare the results of the previous equation to extensive numeric calculations done directly over a lattice with $L = 10\,000$ varying p. The agreement is quite good for the range of interest both in values and in slope.

A similar analysis can be done for each of the jamming functions for the whole lattice: $S^k(p)$, $T^k(p)$, $F^k(p)$, $R^k(p)$, and $A^k(p)$. In Fig. 10, we plot the projected results within the range of interest. Here we have omitted the oscillatory behavior for the interacting depositions, which would render the lines presented in Fig. 9 into bands of decreasing width as p decreases. It is noteworthy that the three noninteracting depositions exhibit a parallel behavior, with all of them decreasing mainly due to the impurity effect. The interacting depositions present different values and slopes, which makes them clearly different over the entire range.

IV. CONCLUSIONS

The oriented deposition of k-mers on a lattice has several interesting features, some of them not previously considered in the literature. On the one hand, the problem can be simplified to deposition on ODLs due to directional orientation established by external conditions. On the other hand, the problem is enlarged due to the presence of impurities that break the lattice into finite segments, which do not allow for treatments that are valid in the thermodynamic limit.

Segments present a distribution that maximizes at short lengths, decaying asymptotically to zero for long lengths (see Fig. 2). The average length $\langle \ell(p) \rangle$ decreases with the impurity concentration p, slightly modulated by the lattice length L. For small enough impurity concentrations (around and under 0.1), the weak L dependence can be ignored, giving a direct relationship between $\langle \ell \rangle$ and p [see Eq. (4)].

Three complementary mechanisms contribute to the jamming condition: (a) the impurity concentration p by itself (independent of k and the deposition method); (b) the segments with length under k (also independent of the deposition method); and (c) the jamming within the individual segments (depending on p through $\langle \ell \rangle$ and depending on the deposition conditions generically denoted as γ_ℓ^k). The role of (a) and (b) is summarized by Eq. (9), while function γ_ℓ^k has to be obtained separately for finite values of ℓ according to the deposition mechanism under consideration.

Depositing linear polymers can be interacting or noninteracting. For the latter, three deposition conditions were considered and fully discussed. The configurational method is based on equilibrium conditions yielding the segment jamming function ϕ_ℓ^k, which gives the highest values among

the noninteracting depositions. The sequential irreversible mechanism is based on partial coverage of the configuration space following the irreversible occupations leading to the jamming function θ_ℓ^k with values under those for ϕ_ℓ^k. The baseline method is based on the jamming configurations only leading to σ_ℓ^k, which presents the lowest jamming values. This functional dependence of the deposition of noninteracting k-mers with ℓ is summarized by the central three curves in Fig. 6.

The interacting depositions present commensuration effects that are more noticeable for shorter segments (or higher impurity content). The repulsive deposition is characterized by the function $\gamma_\ell^k \to \rho_\ell^k$, which presents decreasing oscillations of period $2k-1$ around a value $k/(2k-1)$. Repulsion among segments means the largest possible empty intersegment spacings. This leads to the lowest possible values in Fig. 6. On the other extreme is the attractive depositions characterized by the function $\gamma_\ell^k \to \alpha_\ell^k$, which presents decreasing oscillations with the highest values always 1.0, corresponding to cases of jamming by $n = \ell/k$ k-mers, with n an exact integer number. In this case we reach the maximum possible values for the jamming values in Fig. 6.

It is interesting to notice that numeric simulations based on irreversible depositions produce a dispersion of results that span a range of jamming values that include the three noninteracting depositions (see Fig. 7). This means that some of the irreversible depositions find the low probability path to exhibit coverage close to the high values of the configurational deposition. On the other extreme, some irreversible depositions go over mostly jamming configurations staying close to the low values of the baseline method.

The dependence of the jamming functions with the length of the k-mer has two different components. On one side, there is a monotonous decrease of the lattice available for depositions as k grows, as can be seen in Fig. 4. On the other side, there is a nonmonotonic oscillatory behavior for high p values as k grows in the way illustrated by Fig. 8.

We can obtain linear regressions for previous γ functions in the low-p regime. This result is combined with the fraction of the whole lattice L actually available for depositions given by Eq. (9), which is common to all deposition methods. This was done explicitly for the case of $T^k(p)$ by means of θ_ℓ^k, which allows the method to be tuned to establish the relationship between $\langle\ell\rangle$ and p (see Fig. 9).

The extension of this projection method to the other deposition cases allows us to obtain similar projected jamming functions for all of them, as is shown in Fig. 10. The order is $A^k(p) > F^k(p) > T^k(p) > S^k(p) > R^k(p)$ in general terms. However, some of the slopes are different, so some discrepancies to previous ordering could be found out of the range considered here for p. This picture will be more complicated as the length of the polymers increases.

Most of the reported calculations were done for trimers. However, the extension to other k-mers is straightforward. The case of dimers is actually simpler than the one for trimers reaching higher values for all jamming functions (see Fig. 8). The case of longer k-mers requires special care for high impurity content as oscillations are strong, as can be seen for the case $k = 4$ in Fig. 8. For a particular application involving a polymer of given length over 4, a special study has to be conducted with the appropriate deposition method.

ACKNOWLEDGMENTS

This work was supported in part by CONICET (Argentina) under Project No. PIP 112-201101-00615, Universidad Nacional de San Luis (Argentina) under Project No. 322000, and the National Agency of Scientific and Technological Promotion (Argentina) under Project No. PICT-2013-1678. Most of the numerical work was done using the BACO parallel cluster (composed by 50 PCs each with an Intel i7-3370/2600 processor) located at Instituto de Física Aplicada, Universidad Nacional de San Luis–CONICET, San Luis, Argentina. One of us (E.E.V.) is grateful to Fondecyt (Chile) under Contract No. 1150019, and the Center for the Development of Nanoscience and Nanotechnology (CEDENNA) funded by Conicyt (Chile) under Contract No. FB0807 for partial support.

APPENDIX

In this appendix, we deal with the jamming functions for segments of finite length ℓ, which is one of the parameters to be varied. Let us recall that it is related through the impurity content and the lattice size by Eq. (3). In addition, the size of the k-mer is also a possible variable. We shall use short k-mers here, namely $k = 2$, 3, and 4.

The next consideration is for the deposition case, and that is fixed by a predetermined application. We choose to illustrate the process using the neutral baseline deposition, described in Sec. II B 1. The procedure outlined here can be extended to the other cases by just describing the probability depositions accordingly.

To apply Eq. (17) to get σ_ℓ^k, we need in advance all the probability expressions $P_\ell^{n,k}$, where n runs from u the minimum possible number of k-mers leading to jamming, and to z the maximum number of k-mers that can be accommodated in a segment of length ℓ. This is laborious work, which increases with the size of the segment. To illustrate this point, we present in Table I the coefficients $P_\ell^{n,k}$ for a segment with $\ell = 30$ for $k = 2$, 3, and 4.

We can then plot these results with respect to ℓ^{-1} as it is presented in Fig. 8. These results clearly indicate that finite-size

TABLE I. Coefficients $P_\ell^{n,k}$ intended for the calculation of σ_ℓ^k (as indicated in the text) for k-mers on a 1D homogeneous lattice; k ranges from 2 to 4.

n	$k=2$	$k=3$	$k=4$
4	0.0000	0.0000	0.0038
5	0.0000	0.0000	0.4152
6	0.0000	0.0100	0.5536
7	0.0000	0.3617	0.0274
8	0.0000	0.5532	0.0000
9	0.0000	0.0748	0.0000
10	0.0033	0.0003	0.0000
11	0.1487	0.0000	0.0000
12	0.5155	0.0000	0.0000
13	0.3007	0.0000	0.0000
14	0.0315	0.0000	0.0000
15	0.0003	0.0000	0.0000

segments produce nonmonotonic jamming functions for short segments. Such an effect is mainly due to commensuration between the segment length and the k-mer size. This is even more so as k increases. Then for applications to high impurity content (short segments), particular calculations should be done.

[1] J. W. Evans, Rev. Mod. Phys. **65**, 1281 (1993).
[2] R. Erban and S. J. Chapman, Phys. Rev. E **75**, 041116 (2007).
[3] P. L. Krapivsky, S. Redner, and E. Ben-Naim, *A Kinetic View of Statistical Physics* (Cambridge University Press, Cambridge, 2010).
[4] B. Bonnier, M. Hontebeyrie, Y. Leroyer, C. Meyers, and E. Pommiers, Phys. Rev. E **49**, 305 (1994).
[5] N. Vandewalle, S. Galam, and M. Kramer, Eur. Phys. J. B **14**, 407 (2000).
[6] G. Kondrat and A. Pękalski, Phys. Rev. E **63**, 051108 (2001).
[7] N. I. Lebovka, N. N. Karmazina, Y. Y. Tarasevich, and V. V. Laptev, Phys. Rev. E **84**, 061603 (2011).
[8] M. Pawłowska, S. Żerko, and A. Sikorski, J. Chem. Phys. **136**, 046101 (2012).
[9] M. Pawłowska and A. Sikorski, J. Mol. Model. **19**, 4251 (2013).
[10] P. Adamczyk, P. Romiszowski, and A. Sikorski, J. Chem. Phys. **128**, 154911 (2008).
[11] M. Nakamura, Phys. Rev. A **36**, 2384 (1987).
[12] R. D. Vigil and R. M. Ziff, J. Chem. Phys. **91**, 2599 (1989).
[13] R. Dickman, J.-S. Wang, and I. Jensen, J. Chem. Phys. **94**, 8252 (1991).
[14] I. A. Kriuchevskyi, L. A. Bulavin, Y. Y. Tarasevich, and N. I. Lebovka, Condens. Matter Phys. **17**, 33006 (2014).
[15] R. Connelly and W. Dickinson, Philos. Trans. R. Soc. A **372**, 20120039 (2014).
[16] M. Cieśla and J. Barbasz, J. Mol. Model. **19**, 5423 (2013).
[17] J. Feder, J. Theor. Biol. **87**, 237 (1980).
[18] V. Cornette, A. J. Ramirez-Pastor, and F. Nieto, Phys. Lett. A **353**, 452 (2006).
[19] V. Cornette, A. J. Ramirez-Pastor, and F. Nieto, J. Chem. Phys. **125**, 204702 (2006).
[20] Y. Y. Tarasevich, V. V. Laptev, N. V. Vygornitskii, and N. I. Lebovka, Phys. Rev. E **91**, 012109 (2015).
[21] G. Kondrat, J. Chem. Phys. **122**, 184718 (2005).
[22] G. Kondrat, J. Chem. Phys. **124**, 054713 (2006).
[23] T. Yeshua, C. Lehmann, U. Hübner, S. Azoubel, S. Magdassi, E. E. B. Campbell, S. Reich, and A. Lewis, Nano Lett. **16**, 1517 (2016).
[24] N. Sharma, R. A. van Mourik, Y. Yin, B. Koopmans, and S. S. P. Parkin, Nanotechnology **27**, 165301 (2016).
[25] Y. Yao, E. Metwalli, M. A. Niedermeier, M. Opel, C. Lin, J. Ning, J. Perlich, S. V. Roth, and P. Müller-Buschbaum, ACS Appl. Mater. Interf. **6**, 5244 (2014).
[26] G. D. García, F. O. Sanchez-Varretti, P. M. Centres, and A. J. Ramirez-Pastor, Physica A **436**, 558 (2015).
[27] W. Krauth, *Statistical Mechanics: Algorithms and Computations* (Oxford University Press, Oxford, 2006).
[28] V. Privman and P. Nielaba, Europhys. Lett. **18**, 673 (1992).